

# Advanced oxidation protein products promote NADPH oxidase-dependent $\beta$ -cell destruction and dysfunction through the Bcl-2/Bax apoptotic pathway

Min Liang<sup>1,2</sup>, Aiqing Li<sup>1,2</sup>, Aiju Lou<sup>1</sup>, Xifang Zhang<sup>1</sup>, Youyuan Chen<sup>1</sup>, Lei Yang<sup>1</sup>, Yumin Li<sup>1</sup>, Shenglin Yang<sup>1</sup> and Fan Fan Hou<sup>1</sup>

The accumulation of plasma advanced oxidation protein products (AOPPs) has been linked with diverse disorders, including diabetes, chronic kidney disease, obesity, and metabolic syndrome. The aim of the present study was to evaluate the pathophysiological relevance of AOPPs in  $\beta$ -cell destruction and dysfunction. Exposure of cultured rat  $\beta$ -cells (INS-1) to AOPPs induced an increase in Bax expression, caspase-3 activity, and apoptosis as well as a decrease in Bcl-2 expression in a dose- and time-dependent manner. AOPP challenge rapidly increased the production of intracellular superoxide by activation of NADPH oxidases, demonstrated by p47<sup>phox</sup> translocation and interaction with p22<sup>phox</sup> and gp91<sup>phox</sup>, and this in turn led to apoptosis. AOPPs treatment resulted in  $\beta$ -cell apoptosis, AOPPs accumulation, and decreased insulin content in pancreas and plasma in unilateral nephrectomized rats. Chronic inhibition of NADPH oxidase by apocynin prevented  $\beta$ -cell apoptosis and ameliorated insulin deficiency in AOPP-challenged rats. This study demonstrates for the first time that accumulation of AOPPs promotes NADPH oxidase-dependent  $\beta$ -cell destruction and dysfunction by the Bcl-2/Bax–caspase apoptotic pathway. This finding may provide a mechanistic explanation for  $\beta$ -cell destruction and dysfunction in patients with diverse disorders.

*Laboratory Investigation* (2017) **97**, 792–805; doi:10.1038/labinvest.2017.24; published online 6 March 2017

Diabetes mellitus continues to be a major health problem worldwide. It is estimated that 225 million people are affected, and this number is projected to increase to at least 353 million by 2030.<sup>1,2</sup> Diabetes is associated with a dramatically increased risk of heart attack, stroke, and renal failure, as well as disability. The cost of diabetes-related health care was estimated to be \$232 billion in 2007, which represents a major economic burden worldwide.<sup>3</sup> Thus, there is a pressing need to understand the pathogenic mechanisms and develop strategies to prevent the development of diabetes. There is increasing evidence that pancreatic  $\beta$ -cell destruction and dysfunction are the central events in the development and progression of diabetes.<sup>4</sup>  $\beta$ -Cell destruction is associated with a deficiency in insulin secretion,  $\beta$ -cell proliferation disorder and apoptosis. Glucose and free fatty acids are important regulators of  $\beta$ -cell insulin secretion.<sup>5</sup> However, patients with chronic renal failure have a significantly increased risk of developing prediabetes mellitus.<sup>6</sup> Rats with chronic kidney

disease developed insulin deficiency and glucose intolerance.<sup>7</sup> Thus,  $\beta$ -cell destruction and dysfunction cannot be completely explained by prolonged exposure to glucose (glucotoxicity) or fatty acids (lipotoxicity). The mechanisms that underlie  $\beta$ -cell injury remain only partially understood.

Although multiple biochemical pathways and mechanisms of actions to cause  $\beta$ -cell damage have been suggested, they have in common the formation of reactive oxygen species (ROS).<sup>8</sup> Nicotinamide adenine dinucleotide phosphate (NADPH) is a major source of ROS generation in both physiologic and pathophysiologic situations.<sup>9</sup> It is now widely accepted that oxidative stress acts as one of central mechanisms for development of type 2 diabetes.<sup>8,10</sup> ROS can induce dysfunction and apoptosis in pancreatic  $\beta$ -cells.<sup>11</sup> Interestingly, compared with many other cell types, the  $\beta$ -cells may be at high risk for oxidative stress with an increased sensitivity for apoptosis, due to relatively low levels of antioxidant enzymes in islets.<sup>12,13</sup>

<sup>1</sup>State Key Laboratory of Organ Failure Research, National Clinical Research Center of Kidney Disease, Key Clinical Specialty Discipline Construction Program, Division of Nephrology, Nanfang Hospital, Southern Medical University, Guangzhou, PR China

Correspondence: Professor FF Hou, MD, PhD, Division of Nephrology, Nanfang Hospital, 1838 North Guangzhou Avenue, Guangzhou 510515, PR China.

E-mail: ffhouguangzhou@163.com

<sup>2</sup>These two authors contributed equally to this work.

Received 23 September 2016; revised 16 January 2017; accepted 25 January 2017

Recent studies have found that exposure of  $\beta$ -cells to advanced glycation end products, the products of non-enzymatic glycation/oxidation of proteins/lipids, caused a decrease of cellular proliferation and insulin release, as well as an increase of intracellular oxidative stress and cell apoptosis.<sup>14,15</sup> Accumulation of advanced oxidation protein products (AOPPs), a recently identified family of oxidated protein compounds, has been linked with diseases associated with oxidative stress, including diabetes, chronic kidney disease, obesity, and metabolic syndrome.<sup>16–19</sup> AOPPs are a family of dityrosine-containing protein products generated by reaction of proteins with hypochlorous acid (HOCl) and mainly carried by albumin *in vivo*.<sup>20</sup> Chronic accumulation of AOPPs worsened renal function and fibrosis in remnant kidney and experimental diabetic nephropathy.<sup>21,22</sup> A previous *in vitro* study showed that AOPPs activated vascular endothelial cells via RAGE-mediated signals involving NADPH oxidase.<sup>15</sup> In chronic kidney disease, AOPPs activated intrarenal renin angiotensin system via a CD36-mediated, redox-dependent pathway.<sup>23</sup> Together, these studies suggested that AOPPs might be a class of redox-sensitive pathogenic mediators. However, there is a lack of studies investigating the pathogenic effects of AOPPs on islet cells.

This study was conducted to test the hypothesis that AOPPs may trigger  $\beta$ -cell destruction and dysfunction of insulin secretion in diabetes. We demonstrated that, both *in vitro* and *in vivo*, AOPPs triggered  $\beta$ -cell apoptosis and impaired insulin secretion. AOPPs increased ROS generation. NADPH oxidase-dependent oxidative stress mediated  $\beta$ -cell dysfunction and apoptosis. These results revealed a new mechanism underlying  $\beta$ -cell destruction and dysfunction.

## MATERIALS AND METHODS

### AOPPs Preparation

AOPP-RSA was prepared *in vitro* as described previously.<sup>15,23</sup> Briefly, fatty acid-free RSA (Sigma Chemical, St Louis, MO, USA) was exposed to 200 mmol/l HOCl (Fluke, Buchs, Switzerland) for 30 min in the absence of free amino acid/carbohydrate/lipids. The preparation was dialyzed overnight against phosphate-buffered saline to remove free HOCl. AOPPs content were determined by measuring absorbance at 340 nm in acidic condition and were calibrated with chloramines-T in the presence of potassium iodide.

### AOPP Monoclonal Antibody Preparation

Monoclonal antibodies against AOPPs (Clone 3F2) were generated as described previously.<sup>24</sup> Briefly, the ascites were purified by affinity chromatography using HiTrap protein G Hp (GE Healthcare Bioscience, Piscataway, NJ, USA). The monoclonal antibody isotypes were determined using a Monoclonal Antibody Isotype Kit (Pierce, Rockford, IL, USA).

### Cell Culture

Rat pancreatic  $\beta$  cell lines (INS-1) were cultured in RPMI-1640 medium (Gibco, Grand Island, NY, USA) with 11 mmol/l D-glucose supplemented with 10% fetal calf serum (Gibco), 100 U/ml penicillin, 100 g/ml streptomycin, 10 mmol/l HEPES, 2 mmol/l L-glutamine, 1 mmol/l sodium pyruvate and 50  $\mu$ mol/l  $\beta$ -mercaptoethanol (all from Sigma Chemical) at 37 °C in 5% CO<sub>2</sub>. Viability of INS-1 cells was determined by trypan blue dye exclusion test. After 80% confluence was reached, INS-1 cells were depleted in RPMI-1640 medium (Gibco) with 11 mmol/l D-glucose (Sigma Chemical) plus 0.1% bovine serum albumin (Sigma Chemical) for 24 h, and then treated with AOPPs with the indicated concentration and time.

### Islet Purification, Culture and Secretion

#### Islet isolation and culture

All animal procedures were approved by the Animal Experiment Committee of Nanfang Hospital. Islet isolation and culturing has been performed as described previously.<sup>25</sup> Male Sprague-Dawley rats weighing 250–300 g were used for islet isolation. Briefly, the pancreatic islets were digested and isolated by perfusing collagenase P via the pancreatic duct and purified by discontinuous Ficoll-400 density gradients. Islets were cultured in RPMI-1640 medium (Gibco) with 11 mmol/l D-glucose supplemented with 10% fetal calf serum, 100 U/ml penicillin, 100 mg/ml streptomycin, 10 mmol/l HEPES, 2 mmol/l L-glutamine, 1 mmol/l sodium pyruvate, and 50  $\mu$ mol/l  $\beta$ -mercaptoethanol (all from Sigma Chemical). Two days after plating, islets become flattened and treated with AOPPs with the appropriate concentrations.

#### Glucose-stimulated insulin secretion

Fifty size-matched islets were pre-incubated for two sequential periods of 2 h at 37 °C in Krebs–Ringer bicarbonate buffer (3.6 mmol/l KCl, 135 mmol/l NaCl, 1.5 mmol/l CaCl<sub>2</sub>, 5 mmol/l NaHCO<sub>3</sub>, 0.5 mmol/l NaH<sub>2</sub>PO<sub>4</sub>, 0.5 mmol/l MgCl<sub>2</sub>, 10 mmol/l HEPES) containing 3.3 mmol/l or 16.7 mmol/l glucose with 0.5% bovine serum albumin. The supernatants were collected and centrifuged at 13 000 g for 2 min. Insulin was measured in the supernatant *via* ELISA (Merckodia, Uppsala, Sweden).

### Animal Model

Male Sprague-Dawley rats (initial weight 200–220 g, Nanfang Hospital Animal Experiment Center) were fed with standard rat chow *ad libitum* and given free access to water. The rats were subjected either to UNX or to sham operation (sham). One week after the operation, the UNX rats were randomized into four groups ( $n=6$  in each group) and received daily intravenous injection of vehicle (endotoxin-free PBS, pH 7.4), native RSA (50 mg/kg per day), AOPP-RSA (50 mg/kg per day), or AOPP-RSA (50 mg/kg per day) plus intragastric administration of apocynin (10 mg/kg per day; Sigma Chemical) for 8 weeks. UNX removes one kidney and

decreases the glomerular filtration rate, thereby effectively causing AOPP accumulation in the plasma and pancreas. All animal experiments were approved by the Animal Ethics Committee of Nanfang Hospital.

Plasma insulin was measured by commercial rat insulin ELISA kit (Mercodia). Serum creatinine was measured by an automatic biochemical analyzer (AU480; Beckman Coulter). The 24-h urinary protein excretion was measured using the Coomassie Blue method.<sup>26</sup>

### Assessment of $\beta$ -Cell Apoptosis

#### *Annexin V-FITC/PI staining experiment*

INS-1 cell apoptosis was detected with an Annexin V-FITC Apoptosis Detection Kit (Invitrogen, Carlsbad, CA, USA) according to the manufacturer's protocol. Briefly, treated cells were harvested by trypsin, washed twice with PBS, and were then re-suspended in binding buffer at a concentration of  $1 \times 10^5$  cells/ml according to the manufacturer's instruction. Cells were stained with either fluorescein isothiocyanate (FITC)-conjugated Annexin V-alone, propidium iodide (PI) alone, or a combination of both according to the manufacturer's instructions (Invitrogen). The apoptotic index was immediately determined by flow cytometry. All early apoptotic cells (Annexin V-alone), necrotic (PI-alone), late apoptotic cells (double positive) as well as living cells (double negative) were analyzed by FACSCalibur and Cell Quest software (BD FACSCalibur System, Franklin Lakes, NJ, USA). Argon laser excitation wavelength was 488 nm, while emission data were acquired at wavelength 525 nm for FITC and 620 nm for PI.

#### *Fluorescent TdT-mediated dUTP nick-end labeling assay*

DNA strand breaks in INS-1 cells were identified using *in situ* TdT-mediated dUTP nick-end labeling (TUNEL) (Roche Diagnostic, Penzberg, Germany) according to the method described previously and the manufacturer's instructions.<sup>27</sup> The cells were fixed in 4% paraformaldehyde followed by methanol. After washing, cells were incubated in TdT buffer containing the TdT enzyme and FITC-conjugated dUTP according to the manufacturer's protocol (Roche Diagnostic), and then counterstained with Hoechst 33258 (Sigma Chemical) according to the manufacturer's protocol. The slides were examined by fluorescent microscopy (Leica TCS SP2 AOBS; Leica Microsystems, Cambridge, UK).

#### *Transmission electron microscopy*

A transmission electron microscopy study was performed as follows: INS-1 cells were fixed with 2.5% glutaraldehyde buffered with 0.1 M sodium phosphate buffer (pH 7.4), post-fixed with 1% OsO<sub>4</sub> in the same buffer for 1 h, and stained with 3% aqueous uranylacetate for 1 h. After dehydration with increasing concentrations of ethanol, the cells were embedded in 6–8 epoxide resin. Ultra-thin sections mounted on copper grids were stained with 3% aqueous uranylacetate and Reynolds' lead citrate for 5 and 3 min, respectively, then

examined under transmission electron microscopy (Hitachi, Tokyo, Japan).

#### *Expression of apoptosis-related molecules*

To measure the protein expression of apoptosis-related molecules, cultured INS-1 cells were lysed and processed for protein extraction. The protein samples were subjected to 8–12% SDS-PAGE before being transferred into polyvinylidene fluoride membranes (NEN Life Science Products, Boston, MA, USA). Western blotting was performed as described<sup>26</sup> using the following primary antibodies: rabbit anti-Bcl-2, anti-Bax, anti-Caspase-3, anti-cleaved Caspase-3 and anti- $\beta$ -actin antibodies (all from Cell Signaling Technology, Beverly, MA, USA). Bound primary antibodies were detected with horseradish peroxidase (HRP)-labeled anti-rabbit secondary antibodies, and visualized using enhanced chemiluminescence reagents (Pierce Chemical, Bockford, IN, USA).

To measure the mRNA levels of apoptosis-related molecules, total RNA was extracted from INS-1 using TRIzol reagent (Invitrogen). An aliquot of each RNA extraction was reverse-transcribed into cDNA using PrimeScript RTase, according to the manufacturer's protocol (TaKaRa Biotechnology, Dalian, China). Real-time PCR was performed in a total volume of 25  $\mu$ l in duplicate by using the TaKaRa SYBR Premix Ex Taq™ kit (TaKaRa Biotechnology) and the Fast Real-Time PCR system 7300 (Applied Biosystems, Carlsbad, CA, USA). The following sets of primers were used: rat GAPDH, forward: 5'-GGACCAGTTGTCTCCTGTG-3', reverse: 5'-TGTAGGCCATGAGGTCCAC-3'; Bcl-2, forward: 5'-GGAGAACAGGGTATGATAACCG-3', reverse: 5'-GGAG TCTTCATCTCCAGTATCCC-3'; Bax, forward: 5'-GGTTGC CCTCTTCTACTTTGCT-3', reverse: 5'-TCCAGTGTCC AGCCCATGA-3'. Relative quantification of each gene was calculated after normalization to GAPDH mRNA by using the  $2^{-\Delta\Delta CT}$  method. The results were shown as a percentage change in expression with respect to unstimulated cells.

#### **Estimation of NADPH Oxidase Activity**

##### *NADPH-dependent generation of ROS*

Intracellular ROS was determined by measuring the fluorescence intensity of the intracellular fluoroprobe 5-(6)-chloromethyl-2',7'-dichlorodihydrofluorescein diacetate (DCFDA; Molecular Probe, Carlsbad, CA, USA).<sup>15</sup> Briefly, rat islet cells were pre-incubated with 1 nmol/l of DCFDA for 30 min. The cells were then incubated with various concentrations of AOPPs for 30 min or with 200  $\mu$ g/ml of AOPPs for the indicated time. One-milliliter aliquots of the cells were removed for fluorescence intensity analysis on a flow cytometry (BD FACSCalibur System). To verify the sources of ROS production, cells were pre-treated for 1 h at 37 °C with NADPH oxidase inhibitor apocynin (10  $\mu$ mol/l) or a O<sub>2</sub>-scavenger that can enter the cells and reduces intracellular ROS (c-SOD, 200 U/ml) (all from Sigma Chemical).

### NADPH-dependent $O_2^-$ production

The levels of intracellular NADPH-dependent  $O_2^-$  production was assessed by chemiluminescence of lucigenin (bis-*N*-methylacridinium nitrate; Sigma Chemical) as described previously.<sup>22</sup> INS-1 cells were incubated with various concentrations of AOPP for indicated time. To verify the sources of  $O_2^-$  production, cells were pre-treated for 1 h at 37 °C with NADPH oxidase inhibitors (diphenyleioidonium, DPI, 100  $\mu$ mol/l; apocynin, 10  $\mu$ mol/l), a nitric oxide synthase inhibitor (*N*<sup>4</sup>-nitro-*L*-arginine methyl ester, *L*-NAME, 10  $\mu$ mol/l), a xanthine oxidase inhibitor (oxypurinol, 100  $\mu$ mol/l), a mitochondria complex I inhibitor (rotenone, 250  $\mu$ mol/l), a mitochondria complex II inhibitor thenoyltri-fluoroacetone (TTFA, 10  $\mu$ mol/l), a mitochondria complex III inhibitor (myxothiazol, 10  $\mu$ mol/l) and a  $O_2^-$  scavenger (c-SOD, 200 U/ml) (all from Sigma Chemical), respectively. The experiments were then repeated as described above. Cell homogenate (100  $\mu$ g/well) were added into a 96-well microplate. Immediately before recording, dark-adapted lucigenin (5  $\mu$ mol/l) with or without NADPH (100  $\mu$ mol/l) were added to cell homogenates. Light emission was recorded every minute for 30 min (VICTOR V Wallac 1420; PerkinElmer, Turku, Finland). Data were expressed as counts per second (c.p.s.).

### Interaction of p47<sup>phox</sup> with p22<sup>phox</sup> and gp91<sup>phox</sup>

The interaction of p47<sup>phox</sup> with p22<sup>phox</sup> and gp91<sup>phox</sup> in cultured INS-1 cells was analyzed by immunoblotting as described previously.<sup>23</sup> The immunocomplexes were obtained by incubation of cell lysates with a rabbit anti-p47<sup>phox</sup>, a rabbit anti-p22<sup>phox</sup>, and a goat anti-gp91<sup>phox</sup> antibody (all from Santa Cruz Biotechnology, Santa Cruz, CA, USA) separately. Immunoblotting was performed using the rabbit anti-rat p47<sup>phox</sup> antibody (1:1000; Santa Cruz Biotechnology) as the primary antibody and the HRP-conjugated swine anti-rabbit or anti-goat IgG (DakoCytomation, Glostrup, Denmark) as the secondary antibody. The membranes were detected by ECL (Pierce Chemical). To determine the total p47<sup>phox</sup>, p22<sup>phox</sup>, or gp91<sup>phox</sup>, the membranes were eluted and incubated with the anti-rat p47<sup>phox</sup> (1:1000), p22<sup>phox</sup> (1:1000), or gp91<sup>phox</sup> (1:1000) antibodies and then detected with the HRP-conjugated anti-rabbit or anti-goat IgG antibody (DakoCytomation).

### P47<sup>phox</sup> membrane translocation

Cultured INS-1 cells were fixed in 4% paraformaldehyde. After washing and blocking, the cells were incubated with a rabbit anti-rat p47<sup>phox</sup> monoclonal antibody overnight at 4 °C. After washing, the slides were incubated with FITC-conjugated goat anti-rabbit immunoglobulins (DakoCytomation) for 45 min at 37 °C, washed, stained with PI (Sigma Chemical) and observed under a confocal microscopy (Leica TCS SP2 AOBS; Leica Microsystems, Cambridge, UK).

### Immunohistochemistry

Paraffin sections were cut at 4  $\mu$ m, deparaffinized and microwaved in 10 mM citrate buffer (pH 6.0) at 100 °C for 5 min to unmask the antigen. After blocking the endogenous peroxides, the sections were subsequently incubated with an anti-AOPP or guinea pig anti-insulin polyclonal antibody (Gene Tech, Shanghai, China) at 4 °C overnight. Finally, the slides were visualized by diaminobenzidine using the REAL EnVision Detection Kit (Dako, Glostrup, Denmark), following the manufacturer's instructions. All sections were counterstained with hematoxylin. An image of each section was captured using a light microscope (Olympus, Tokyo, Japan). The integrated optical density of positively stained islets from three sections was determined for each rat using Image-Pro Plus 7.0 Software (Media Cybernetics, Silver Spring, MD, USA) with the integrated optical density corrected for background. A total of 20 islets per group ( $n = 6$  rats/group) were analyzed.

### Histological Analyses

Four-micrometer paraffin pancreata sections were cut, deparaffinized, blocked in 5% bovine serum albumin, and incubated with a guinea pig anti-insulin polyclonal antibody (Gene Tech) overnight at 4 °C, and reacted with a FITC-conjugated swine anti-guinea pig immunoglobulins for 30 min at 37 °C. The slides were then stained with TUNEL (Roche Diagnostic) and Hoechst 33258 (Sigma Chemical), and observed under the confocal microscopy (Leica Microsystems).

### Statistical Analysis

All data were expressed as mean  $\pm$  s.d. Continuous variables between groups at each time point were compared using a one-way analysis of variance, followed by an LSD method when  $P < 0.05$ . Differences of the variables between two time points were determined by independent samples *t*-test. The relationship between variables was assessed by the Pearson correlation analysis. Statistical analyses were conducted with SPSS 13.0 for Windows (SPSS, Chicago, IL, USA).  $P < 0.05$  was considered statistically significant.

## RESULTS

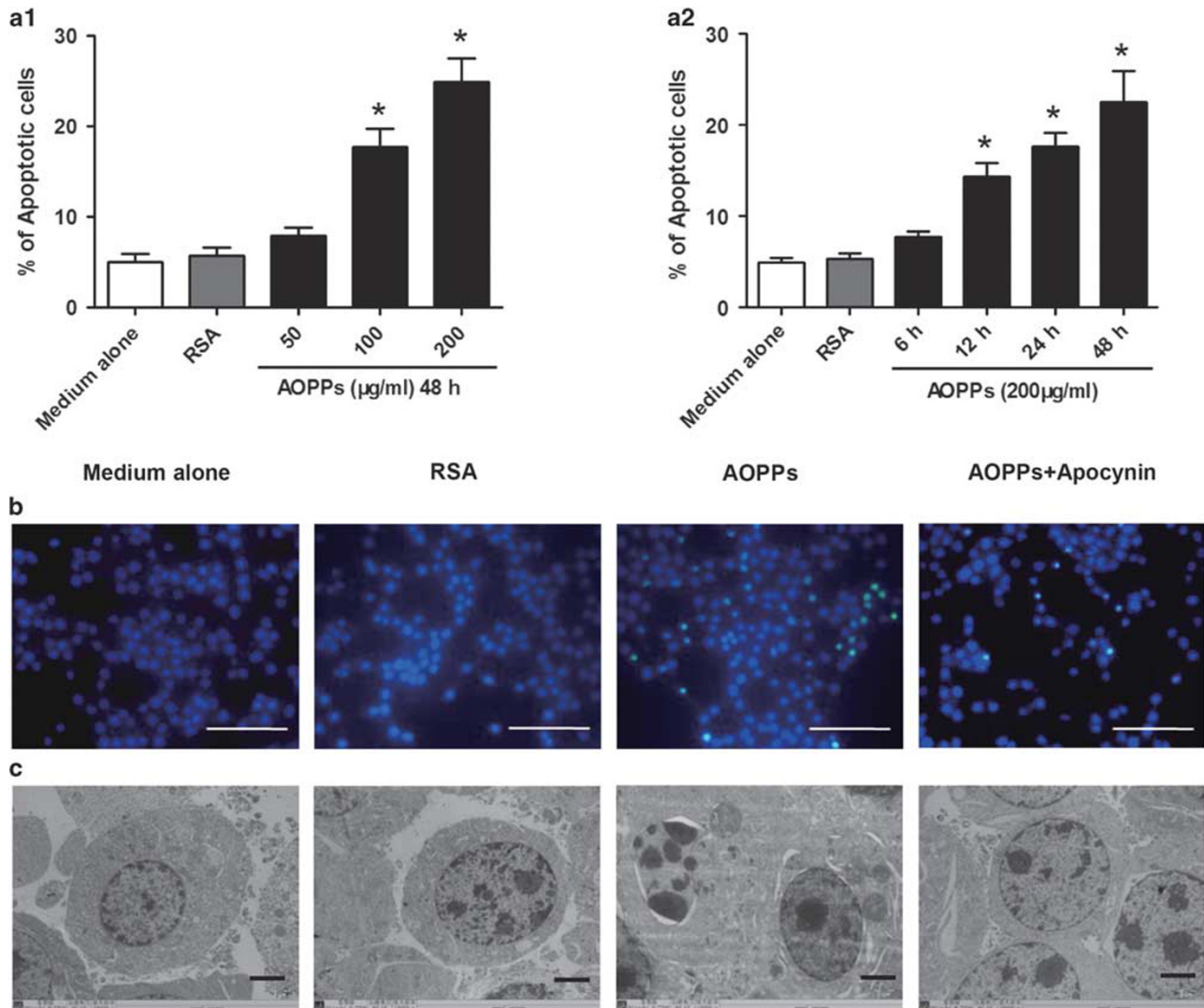
### AOPP-Triggered Apoptosis of $\beta$ -Cells *In Vitro* was Associated with Increased Bax Protein Synthesis and Caspase-3 Activity as Well as Decreased Bcl-2 Protein Synthesis

To determine whether AOPPs accumulation induces  $\beta$ -cell apoptosis, cultured INS-1 cells were incubated with the indicated concentration of AOPP-rat serum albumin (RSA) for 48 h or treated with 200 mg/ml of AOPP-RSA for the indicated time. Exposure of  $\beta$ -cells to AOPP-RSA induced a dose- and time-dependent increase in apoptosis as assessed by Annexin V-labeled cells (Figure 1a1 and a2). Increased apoptosis in INS-1 cells incubated with AOPP-RSA was also shown by analysis of DNA strand breaks with the TUNEL assay (Figure 1b) and electron microscopic analysis

(Figure 1c). AOPP-induced apoptosis could be largely blocked by treatment of apocynin, indicating that the apoptotic processes are dependent on the activation of NADPH oxidase (Figure 1b and c).

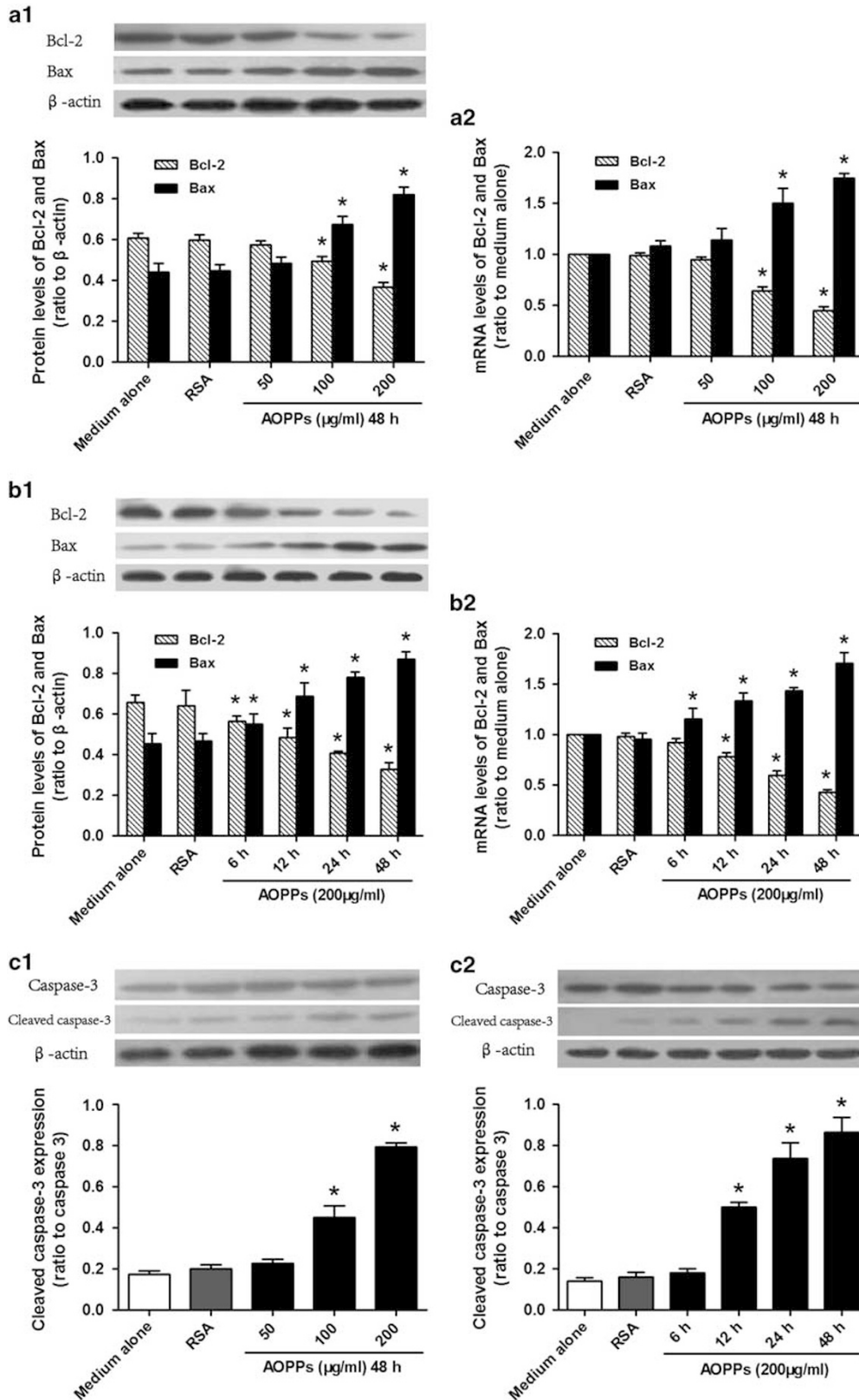
To examine the potential mediators of AOPP-induced apoptosis, we analyzed the abundance of Bcl-2 family proteins

(Bcl-2 and Bax) and caspase-3 by western blot analysis. AOPP-RSA incubation induced a decrease in antiapoptotic Bcl-2 expression and an increase in proapoptotic Bax at both protein and mRNA levels in a dose-dependent manner (Figure 2a1 and a2). AOPPs challenge decreased both protein and mRNA levels of Bcl-2 in INS-1 cells from 6 h (Figure 2b1 and b2).



**Figure 1** Advanced oxidation protein products (AOPPs) triggered apoptosis in cultured pancreatic  $\beta$ -cells. (a) Cultured INS-1 cells were incubated with an indicated concentration of AOPP-RSA for 48 h (a1) or treated with 200  $\mu$ g/ml of AOPP-RSA for the indicated time (a2). Apoptotic  $\beta$ -cells, determined by Annexin V labeling, significantly increased in a dose- and time-dependent manner. Data are expressed as mean  $\pm$  s.d. ANOVA;  $P < 0.05$ ;  $*P < 0.05$  vs medium alone. (b) Representative photographs showing Hoechst 33258- (blue) and TUNEL (TdT-mediated dUTP nick-end labeling)-positive (green) apoptotic cells in cultured INS-1 cells. Scale bar, 50  $\mu$ m. (c) Representative electron micrographs of  $\beta$ -cells incubated with or without AOPP-RSA. Scale bar, 1  $\mu$ m.

**Figure 2** Advanced oxidation protein products (AOPPs) challenge decreased Bcl-2 protein synthesis and increased Bax protein synthesis and caspase-3 activity. (a) Cultured  $\beta$ -cells were incubated with indicated concentration of AOPP-RSA for 48 h or treated with 200  $\mu$ g/ml of AOPP-RSA for the indicated time. Exposure of  $\beta$ -cells to AOPP-RSA decreased Bcl-2 and increased Bax expression at both protein (a1) and mRNA (a2) levels in a dose-dependent manner. (b) Incubation of  $\beta$ -cells with AOPP-RSA triggered a time-dependent downregulation of Bcl-2 and upregulation of Bax at both protein (b1) and mRNA (b2) levels. (c) AOPPs challenge increased cleaved caspase-3 expression in a dose- (c1) and time-dependent (c2) fashion. Data are shown as mean  $\pm$  s.d. of three independent experiments. One-way ANOVA,  $P < 0.05$ .  $*P < 0.05$  vs medium alone.



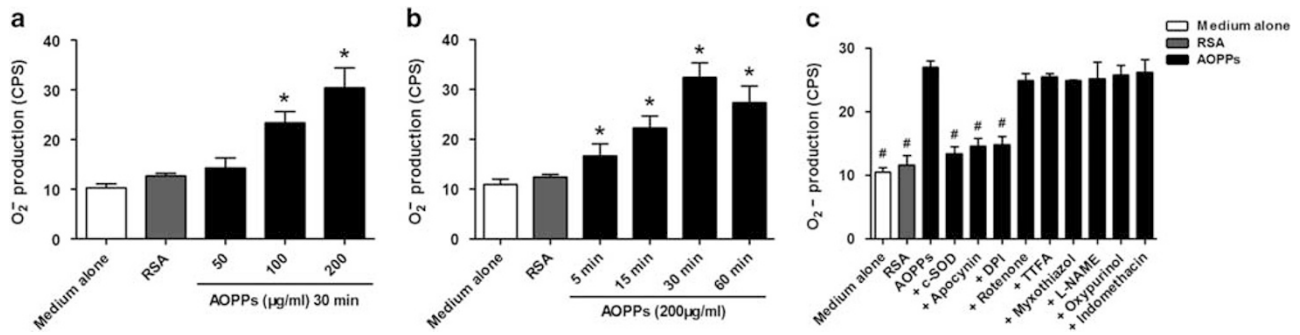


**Figure 3** Advanced oxidation protein products (AOPPs) induced NADPH oxidase-dependent superoxide generation in cultured  $\beta$ -cells. **(a, b)**  $\beta$ -Cells were treated with indicated concentrations of AOPP-RSA or native RSA for 30 min **(a)**, or 200  $\mu\text{g/ml}$  of AOPPs-RSA or 10 mg/ml of native RSA for the indicated time period **(b)**. Cell homogenates were collected, and intracellular superoxide generation was measured by chemiluminescence of lucigenin. **(c)**  $\beta$ -Cells were pre-treated with an  $\text{O}_2^-$  scavenger (c-SOD, 200 U/ml), the inhibitors of NADPH oxidase (DPI, 100  $\mu\text{mol/l}$ , and apocynin, 10  $\mu\text{mol/l}$ ), the inhibitors of mitochondrial respiratory chain complexes (rotenone, 250  $\mu\text{mol/l}$ ; TTFA, 10  $\mu\text{mol/l}$ ; and myxothiazol, 10  $\mu\text{mol/l}$ ), an inhibitor of nitric oxidase (L-NAME, 10  $\mu\text{mol/l}$ ), a xanthine oxidase inhibitor (oxipurinol, 100  $\mu\text{mol/l}$ ), or a cyclooxygenase inhibitor (indomethacin, 10  $\mu\text{mol/l}$ ) before exposure to AOPP-RSA. Intracellular superoxide production was assessed by chemiluminescence of lucigenin. Data are expressed as mean  $\pm$  s.d. ANOVA,  $P < 0.05$ ; \* $P < 0.05$  vs medium alone; # $P < 0.05$  vs AOPPs. c-SOD, cytosolic Cu/Zn superoxide dismutase; DPI, diphenyleneiodonium; L-NAME,  $N^G$ -nitro-L-arginine methyl ester; TTFA, thenoyltrifluoroacetone.

Protein and mRNA levels of Bax increased from 6 h (Figure 2b1 and b2). AOPP-RSA incubation triggered an increase in cleaved caspase-3 in a dose-dependent manner (Figure 2c1). Cleaved caspase-3 increased at 6–48 h of AOPPs treatment (Figure 2c2). These data suggest that AOPP-induced apoptosis is associated with increase activity of the Bcl-2/Bax–caspase-3 pathway.

### AOPPs Challenge Increased NADPH-Dependent Superoxide Generation *In Vitro*

To test the presence of oxidative stress and the enzyme source of superoxide ( $\text{O}_2^-$ ) in AOPP-challenged INS-1 cells, the cells were pre-incubated for 1 h with the inhibitors of various enzymatic systems involved in ROS generation, and an intracellular superoxide ( $\text{O}_2^-$ ) scavenger (cytosolic Cu/Zn superoxide dismutase, c-SOD), respectively. The cells were then incubated with AOPP-RSA for 30 min. NADPH-dependent  $\text{O}_2^-$  production was significantly enhanced in AOPP-treated INS-1 cells in a time- and dose-dependent fashion, compared with cells incubated with medium alone or native RSA (Figure 3a and b). Furthermore, AOPP-triggered  $\text{O}_2^-$  generation was significantly blocked by pre-treating INS-1 cells with c-SOD and NADPH oxidase inhibitors, DPI and apocynin, but not by the inhibitors of nitric oxidase synthase, cyclooxygenase, xanthine oxidase, or the inhibitors of mitochondrial respiratory chain complexes, suggesting that AOPP-triggered  $\text{O}_2^-$  production is dependent on the activation of NADPH oxidase (Figure 3c).

To confirm the presence of oxidative stress and the enzyme source of ROS in AOPP-treated islets, the islets from Sprague-Dawley rats were pre-incubated for 1 h with the  $\text{O}_2^-$  scavenger c-SOD or NADPH oxidase inhibitor apocynin. The cells were then incubated with AOPP-RSA for 30 min. NADPH-dependent ROS production was significantly enhanced in AOPP-treated pancreatic islets in a time- and dose-dependent fashion, compared with cells incubated with

medium alone or native RSA (Supplementary Figure S1). Furthermore, AOPP-triggered ROS generation was significantly blocked by pre-treating islets with c-SOD and apocynin, suggesting that AOPP-triggered ROS production is dependent on the activation of NADPH oxidase (Supplementary Figure S1).

### AOPPs Challenge Activated NADPH Oxidase in INS-1 Cells

To further investigate the mechanisms underlying the induction of  $\text{O}_2^-$  by AOPPs, we examined the effect of AOPPs on the activity of NADPH oxidase. AOPP-RSA induced rapid phosphorylation of the cytoplasmic subunit  $\text{p}47^{\text{phox}}$  in cultured  $\beta$ -cells, with the peak at 30 min (Figure 4a). To examine the interaction of  $\text{p}47^{\text{phox}}$  with the membrane subunits, we immunoprecipitated  $\text{p}22^{\text{phox}}$  and  $\text{gp}91^{\text{phox}}$  with the specific antibodies, and then probed for the coexistence of  $\text{p}47^{\text{phox}}$ . As shown in Figure 4b, the amount of  $\text{p}47^{\text{phox}}\text{-p}22^{\text{phox}}$  complex formation rapidly increased in AOPP-stimulated  $\beta$ -cells. AOPPs also promoted the binding of  $\text{p}47^{\text{phox}}$  with  $\text{gp}91^{\text{phox}}$  (Figure 4c).

The increased expression of NADPH oxidase subunits might be necessary for its sustained activation. To examine the effect of AOPPs on the expression of the oxidase subunits, INS-1 cells were incubated with AOPP-RSA for 6–24 h. Compared with cells incubated with native RSA, INS-1 cells treated with AOPP-RSA showed significantly increased expression of  $\text{p}47^{\text{phox}}$ ,  $\text{p}22^{\text{phox}}$ , and  $\text{gp}91^{\text{phox}}$ , after 6 h of stimulation (Figure 4d). At 30 min after AOPPs challenge,  $\text{p}47^{\text{phox}}$  membrane translocation was apparent (Figure 4e).

### AOPPs Triggered Apoptosis *In Vitro* by NADPH-Dependent Superoxide Generation

To clarify the underlying mechanism of AOPP-induced  $\beta$ -cell apoptosis, INS-1 cells were pre-incubated for 1 h with the  $\text{O}_2^-$

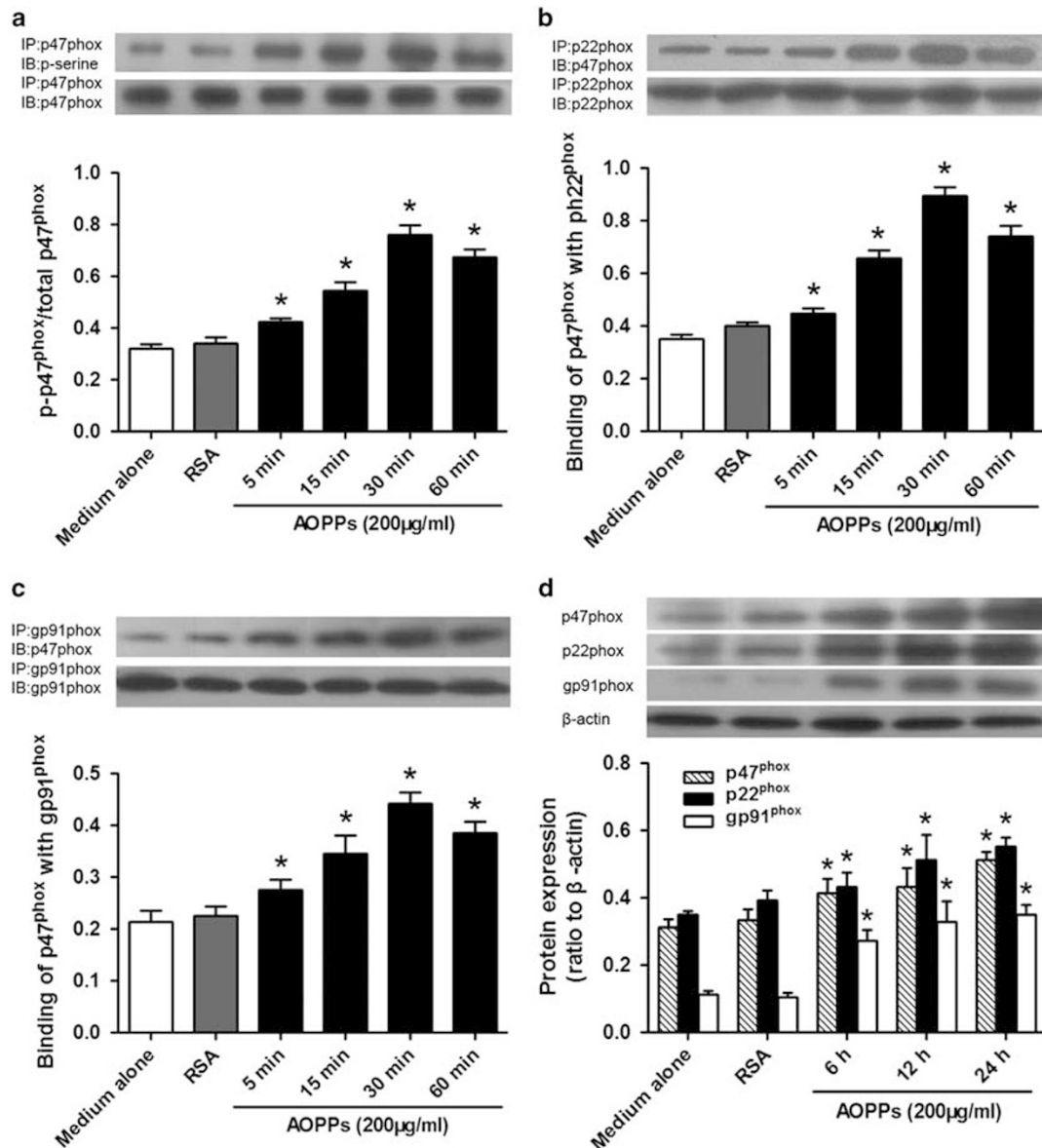


**Figure 4** Advanced oxidation protein products (AOPPs) induced activation of NADPH oxidase in cultured  $\beta$ -cells. (a)  $\beta$ -Cells were incubated with 200  $\mu$ g/ml of AOPP-RSA or native RSA for 5–60 min. Phosphorylation of p47<sup>phox</sup> was assayed by immunoprecipitation (IP) using an  $\alpha$ -p47<sup>phox</sup> and detected by immunoblotting (IB) using an  $\alpha$ -pan-p47<sup>phox</sup> and an  $\alpha$ -phosphoserine as the primary antibodies. (b) AOPP-induced binding of p47<sup>phox</sup> to p22<sup>phox</sup>. Rat  $\beta$ -cells were treated as described above. IP was performed by using an  $\alpha$ -p22<sup>phox</sup> and IB was conducted by using an  $\alpha$ -p47<sup>phox</sup>. (c) Interaction of p47<sup>phox</sup> with gp91<sup>phox</sup>.  $\beta$ -Cells were treated as described above. IP was performed by using an  $\alpha$ -gp91<sup>phox</sup> and IB was conducted by using an  $\alpha$ -p47<sup>phox</sup>. (d) Expression of NADPH oxidase subunits in cultured  $\beta$ -cells.  $\beta$ -Cells were incubated with or without AOPPs for 6–24 h. Protein expression of NADPH oxidase was determined by western blot using the antibodies against the subunits of NADPH oxidase. (e) Representative photographs of AOPPs-induced membrane translocation of p47<sup>phox</sup>.  $\beta$ -Cells were incubated with an  $\alpha$ -p47<sup>phox</sup> and then with an FITC-conjugated secondary antibody and stained with PI. Scale bar, 50  $\mu$ m. Data are expressed as mean  $\pm$  s.d. ANOVA,  $P < 0.05$ ; \* $P < 0.05$  vs medium alone.

scavenger c-SOD and NADPH oxidase inhibitors apocynin and DPI, respectively. The cells were then incubated with AOPP-RSA for 48 h. Downregulation of Bcl-2, upregulation of Bax and activation of caspase-3, could be blocked by the O<sub>2</sub><sup>-</sup> scavenger c-SOD and NADPH oxidase inhibitors apocynin and DPI, which was demonstrated at both protein and mRNA levels (Figure 5a and b). These results suggest that

AOPP-induced activation of proapoptotic molecules is mainly mediated by NADPH oxidase-dependent O<sub>2</sub><sup>-</sup> generation (Figure 5a and b). Similarly, AOPP-induced  $\beta$ -cell apoptosis was significantly suppressed by c-SOD and the NADPH oxidase inhibitors, DPI and apocynin, suggesting that AOPP-triggered  $\beta$ -cell apoptosis is mainly mediated by NADPH oxidase-dependent O<sub>2</sub><sup>-</sup> production (Figure 5c).



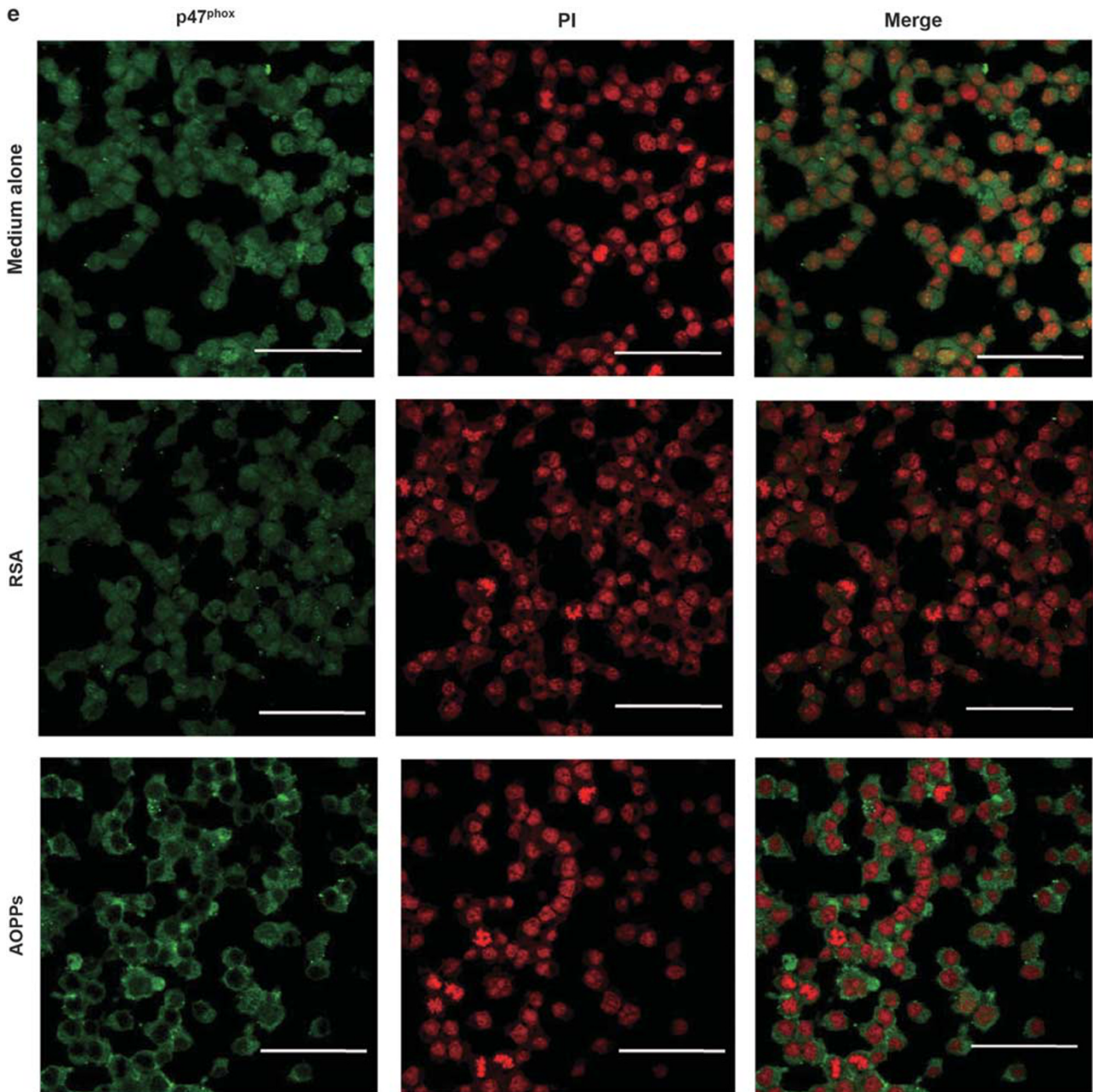


Figure 4 Continued.

### AOPPs Suppressed Glucose-Stimulated Insulin Secretion in Cultured Islets

Treatment of rat islets with AOPPs caused a time- and dose-dependent decrease in insulin secretion at stimulatory (16.7 mM) glucose (Figure 6a and b). RSA treatment did not affect insulin secretion at stimulatory glucose. These data suggest that AOPPs, but not RSA, contribute to suppressed glucose-stimulated insulin secretion. Insulin secretion at stimulatory glucose was preserved by treatment with both the O<sub>2</sub><sup>-</sup> scavenger c-SOD and NADPH oxidase inhibitor apocynin (Figure 6c), indicating that AOPPs-induced

deficiency of insulin secretion depends on the activation of NADPH oxidase.

### AOPPs Accumulation Induced $\beta$ -Cell Destruction in Unilateral Nephrectomized Rats

To verify our *in vitro* finding that AOPPs trigger  $\beta$ -cell destruction, unilateral nephrectomy (UNX) rats were intravenously administered daily with 50 mg/kg of AOPPs with or without apocynin for 8 weeks. AOPPs treatment significantly increased urinary protein excretion in UNX rats relative to that in RSA-treated UNX rats. Apocynin treatment

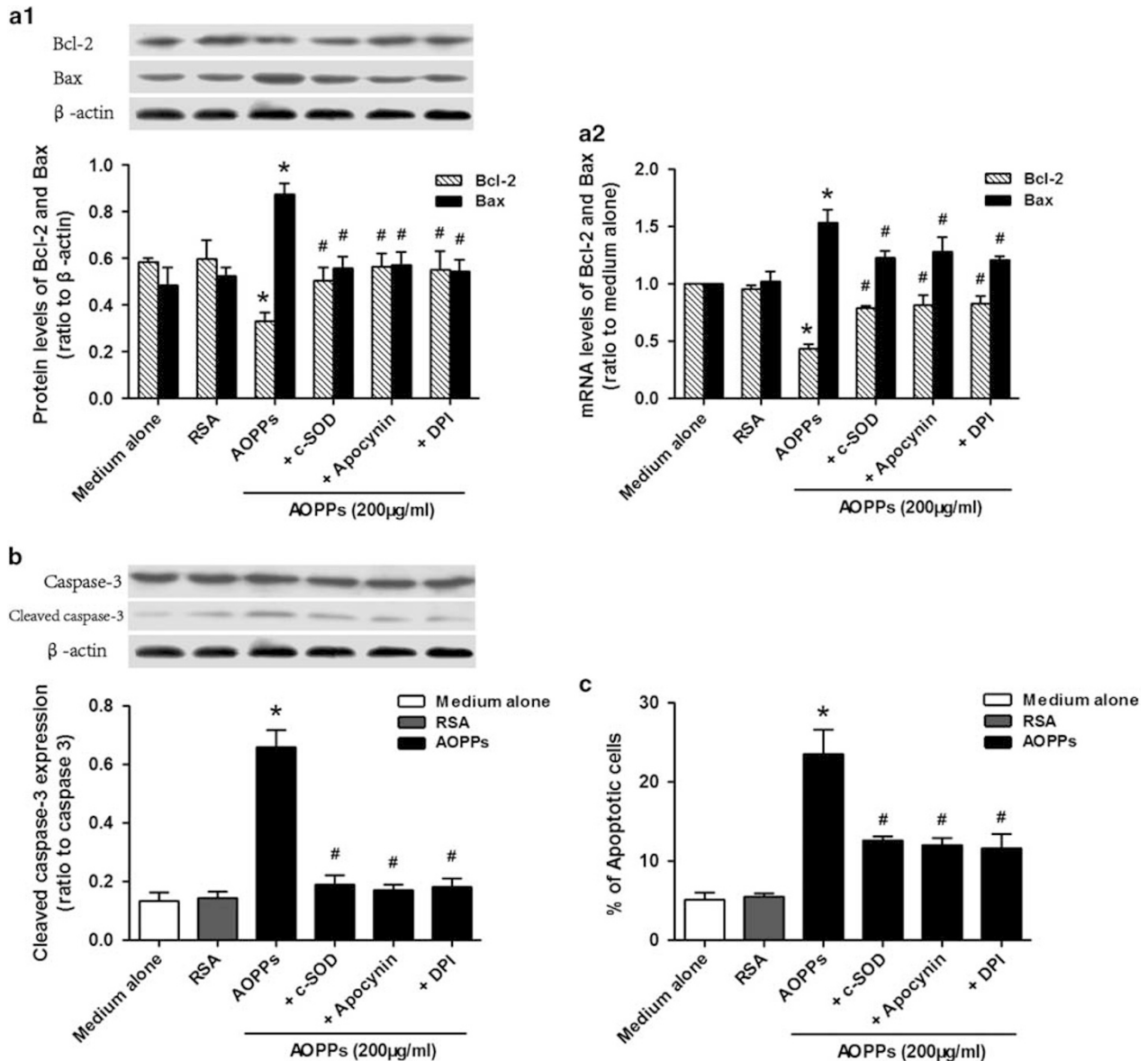


**Figure 5** Advanced oxidation protein products (AOPPs) triggered apoptosis *in vitro* by NADPH-dependent superoxide generation. (a)  $\beta$ -Cells were pre-incubated for 1 h with the  $O_2^-$  scavenger c-SOD and NADPH oxidase inhibitors apocynin and DPI before exposure to AOPP-RSA. Downregulation of Bcl-2 and upregulation of Bax could be blocked by c-SOD, apocynin and DPI at both protein (a1) and mRNA (a2) levels. (b) Activation of caspase-3 could be inhibited by c-SOD, apocynin, and DPI. (c) AOPP-induced  $\beta$ -cell apoptosis, determined by Annexin V labeling, was significantly suppressed by c-SOD, DPI, and apocynin. Data are expressed as mean  $\pm$  s.d. ANOVA,  $P < 0.05$ ; \* $P < 0.05$  vs medium alone; # $P < 0.05$  vs AOPPs. Abbreviation: DPI, diphenyleneiodonium.

ameliorated AOPP-induced urinary protein excretion in UNX animals (data not shown). By a 2-h oral glucose tolerance test, there was significant difference in blood glucose values between AOPP-treated and RSA-treated UNX rats 60, 90 and 120 min, but not at the beginning or 30 min after intragastric administration of 2.5 g/kg glucose (data not shown). Using immunohistochemical analysis, a significant increase of AOPPs expression was detected in pancreas of AOPP-treated UNX rats (Figure 7a1 and a2). Similarly, the AOPP concentration in pancreas homogenates and plasma

significantly increased in AOPP-challenged UNX rats (Figure 7b and c).

The accumulation of AOPPs induced islet cell apoptosis in UNX rats challenged with AOPP-RSA as assessed by triple staining with TUNEL, anti-insulin, and Hoechst. Islet cell apoptosis could be largely blocked by treatment of apocynin (Figure 8a1 and a2). AOPPs treatment significantly decreased the islet insulin content in UNX rats in comparison with that in RSA-treated UNX rats. Apocynin treatment prevented AOPP-induced decreases in islet insulin content (Figure 8b1

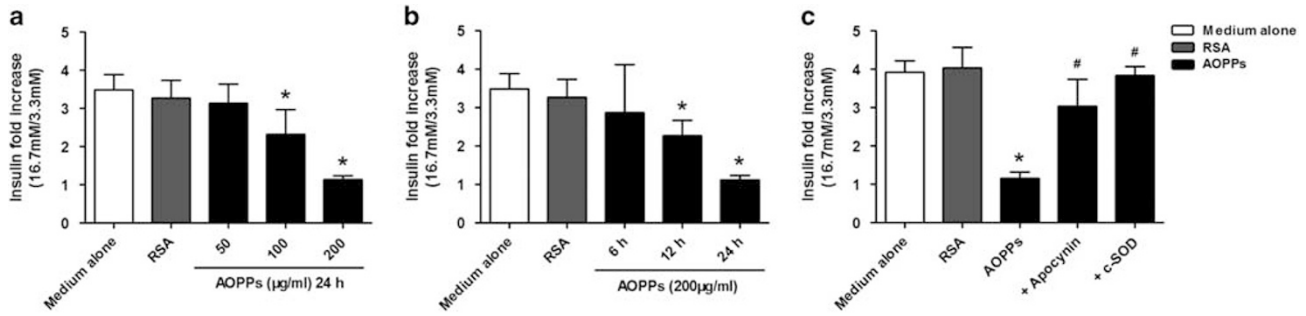


**Figure 6** Advanced oxidation protein products (AOPPs) suppressed glucose-stimulated insulin secretion in cultured islets. (a, b) Rat islets were treated with indicated concentrations of AOPP-RSA or native RSA for 24 h (a), or 200  $\mu$ g/ml of AOPP-RSA or 10 mg/ml of native RSA for the indicated time period (b). Islets were then incubated for two sequential periods of 2 h in Krebs–Ringer bicarbonate buffer containing 3.3 or 16.7 mM glucose. The supernatants were collected and insulin secretion was measured *via* ELISA. (c) Rat islets were pre-treated with an  $O_2^-$  scavenger (c-SOD, 200 U/ml), the inhibitor of NADPH oxidase (apocynin, 10  $\mu$ mol/l) before exposure to AOPP-RSA. Insulin secretion at 16.7 mM glucose relative to 3.3 mM glucose was preserved by treatment with both c-SOD and apocynin. Data are expressed as mean  $\pm$  s.d. ANOVA,  $P < 0.05$ ; \* $P < 0.05$  vs medium alone; # $P < 0.05$  vs AOPPs.

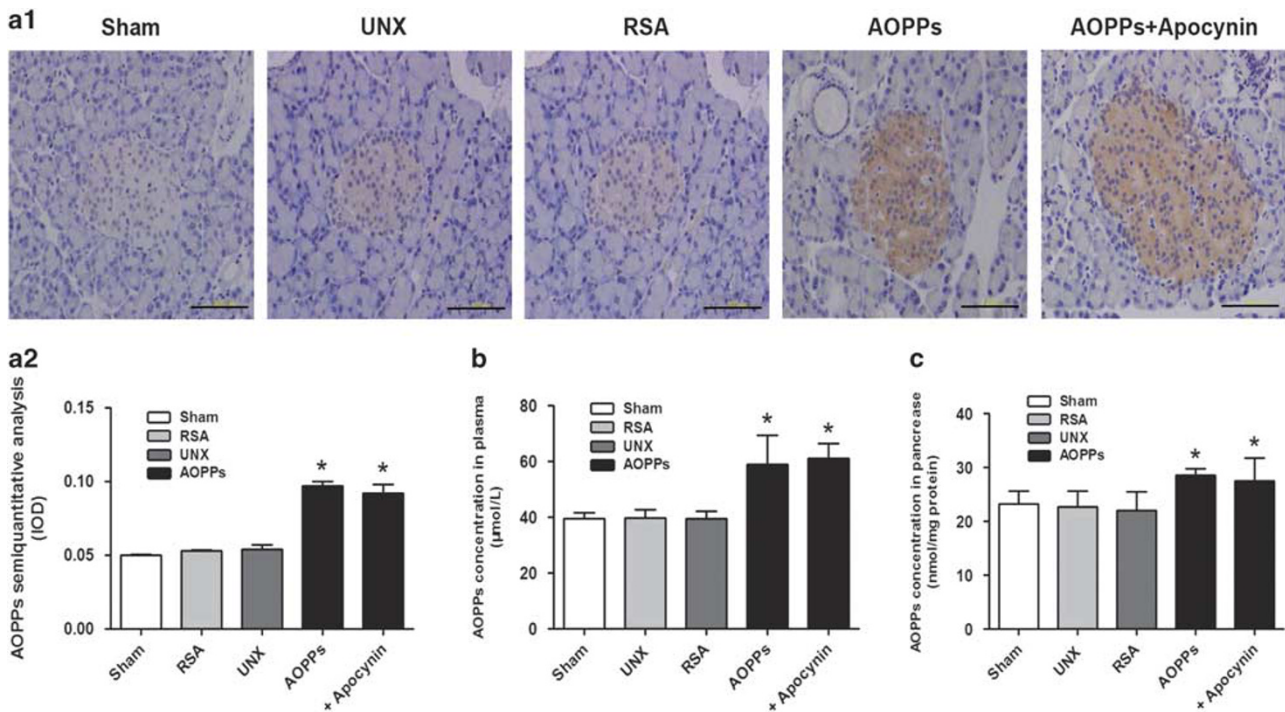


**Figure 7** Advanced oxidation protein products (AOPPs) accumulated in pancreas and plasma in AOPP-challenged unilateral nephrectomized rats. (a) Representative photographs of immunohistochemical staining (a1) and semiquantitative data (a2) of AOPPs expression in AOPP-challenged unilateral nephrectomized (UNX) rats. Scale bar, 100  $\mu$ m. (b) The AOPPs concentration in plasma increased in AOPP-challenged UNX rats. (c) AOPPs concentration in pancreas homogenates increased in AOPP-challenged UNX rats. Data are expressed as mean  $\pm$  s.d. ANOVA,  $P < 0.05$ ; \* $P < 0.05$  vs UNX.

and b2). Similarly, a decrease in insulin concentration in plasma was inhibited by apocynin treatment (Figure 8c).

**DISCUSSION**

Increased recognition of AOPPs, as a class of potential pathogenic mediators and the multiple means by which they form in diverse disorders, including diabetes, chronic kidney disease, obesity, and metabolic syndrome, has highlighted the

importance of determining mechanisms by which AOPPs might induce  $\beta$ -cell destruction and dysfunction. This study provides *in vivo* and *in vitro* evidence showing that the accumulation of AOPPs triggers  $\beta$ -cell apoptosis and results in deficiency of insulin secretion through NADPH oxidase-dependent  $O_2^-$  generation. AOPP-albumin, but not native albumin, altered the life span and function of the  $\beta$ -cells, suggesting that the triggering effect is due to AOPPs and is not

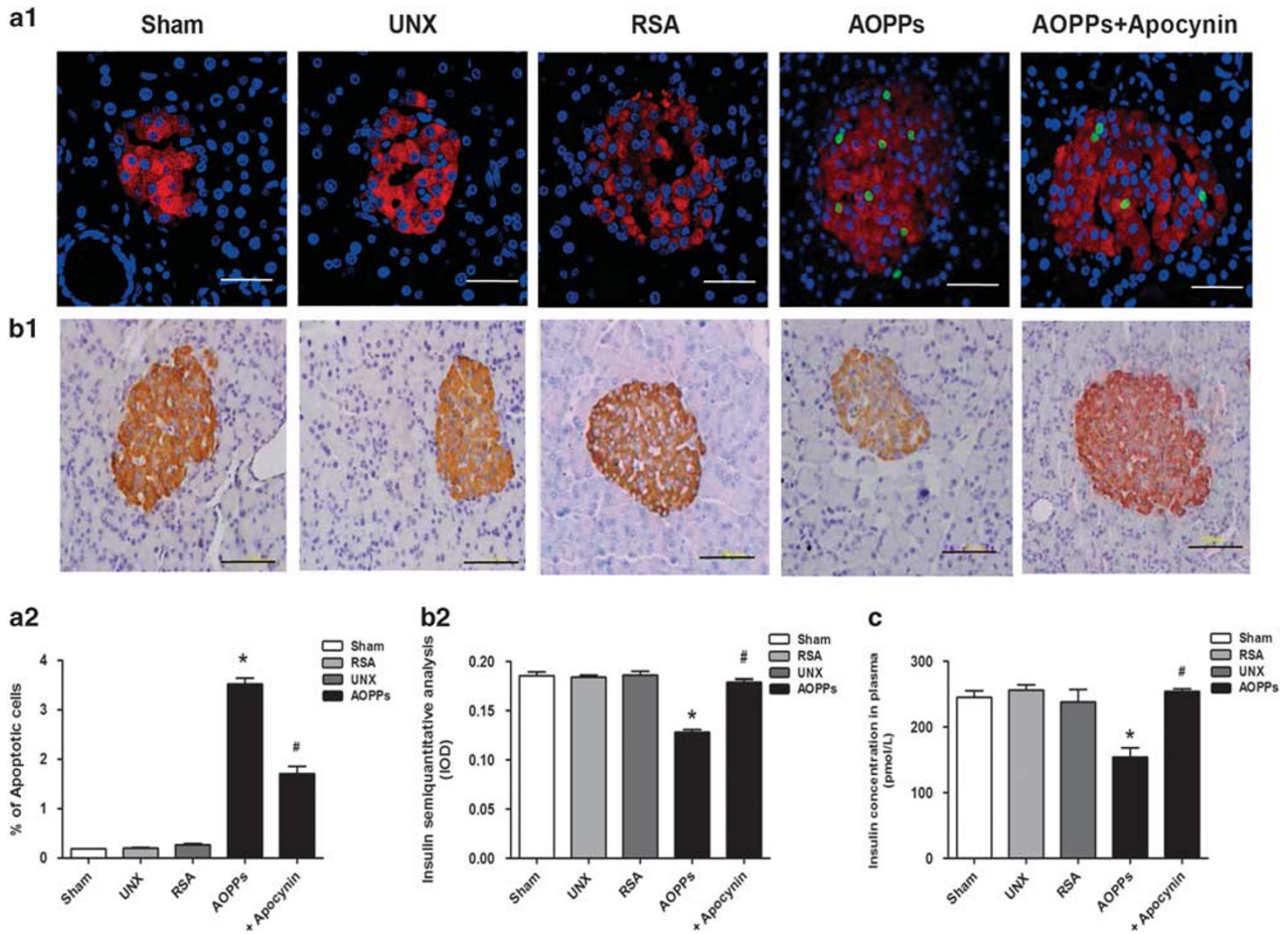


**Figure 8** Advanced oxidation protein products (AOPPs) induced  $\beta$ -cell apoptosis and deficiency of insulin secretion in unilateral nephrectomized rats. (a) AOPP-induced  $\beta$ -cell apoptosis could be largely blocked by treatment of apocynin: representative photographs of pancreas sections stained for TUNEL (TdT-mediated dUTP nick-end labeling) (green), insulin (red), and Hoechst (blue) (a1) and analysis data (a2). Scale bar, 50  $\mu$ m. (b) Apocynin treatment prevented AOPP-induced decreases in islet insulin content: representative photographs of immunohistochemistry staining (b1) and semiquantitative data (b2). Scale bar, 100  $\mu$ m. (c) The insulin content in plasma decreased in AOPP-challenged UNX rats. Data are expressed as mean  $\pm$  s.d. ANOVA,  $P < 0.05$ ; \* $P < 0.05$  vs UNX; # $P < 0.05$  vs AOPPs.

a property of albumin or other contaminants. To the best of our knowledge, this is the first study showing the role of AOPPs in the pathogenesis of  $\beta$ -cell destruction.

Pancreatic  $\beta$ -cell destruction and dysfunction has been known as the central events in the development and progression of diabetes.<sup>4</sup> The mechanisms underlying  $\beta$ -cell destruction have not been completely understood.  $\beta$ -Cell apoptosis is an important mechanism of  $\beta$ -cell destruction and dysfunction.<sup>4</sup> Several factors have been suggested to induce  $\beta$ -cell apoptosis and hasten the progression of  $\beta$ -cell dysfunction; hyperglycemia, free fatty acids, and ROS have been extensively characterized.<sup>28</sup> In this study, we identified AOPPs accumulation as a new candidate mechanism for  $\beta$ -cell apoptosis and deficiency of insulin secretion. It is noteworthy that islet cell apoptosis was increased and insulin deposition in the pancreases was decreased in AOPP-treated rats. Our *in vitro* study also showed that AOPP-RSA triggered  $\beta$ -cell apoptosis in a dose- and time-dependent manner.

AOPPs were also significantly higher in diabetic patients than in controls.<sup>18</sup> Recent studies showed that AOPPs challenge promotes apoptosis and injury in podocytes,<sup>13</sup> renal tubular cells,<sup>29</sup> mesangial cells<sup>30</sup> and vascular endothelial cells,<sup>15</sup> and induce inflammation in THP-1 macrophages.<sup>31</sup> However, this is the first study that AOPPs target islet cells.

Islet  $\beta$ -cells have been shown to express the components of NADPH oxidase including p47<sup>phox</sup>, p22<sup>phox</sup>, and gp91<sup>phox</sup>.<sup>32</sup> NADPH oxidase represents the major source of superoxide generation in  $\beta$ -cells of isolated rodent islets.<sup>12,33</sup> In this study, we showed that AOPPs challenge induced NADPH oxidase-dependent overproduction of  $O_2^-$  in cultured  $\beta$ -cells. AOPPs triggered NADPH-dependent apoptosis through the classic proapoptotic Bcl-2/Bax-caspase pathway in  $\beta$ -cells. These data suggest that NADPH oxidase-dependent  $O_2^-$  generation constitutes a major cause of AOPP-induced  $\beta$ -cell apoptosis. The pathophysiological relevance of NADPH oxidase activation in the induction of pancreatic oxidative

stress has been found in angiotensin II-treated or glucose-treated rat pancreatic islets.<sup>34,35</sup> NADPH oxidase-dependent  $\beta$ -cell apoptosis and dysfunction has been supported in several studies.<sup>2,10,35,36</sup> Oxidative stress is a common response to diseases. AOPPs accumulate in various chronic disease such as diabetes, chronic kidney disease, obesity and metabolic syndrome.<sup>21,22</sup> It had also been shown that increased level of AOPPs correlated with markers of monocyte activation in HIV-positive patients and triggered oxidative burst in human monocytes.<sup>20</sup> Growing evidence show that AOPPs may be not only a marker of oxidant-mediated protein damage, but also a potential inducer of oxidative stress, low-density lipoprotein oxidation, and atherosclerosis.<sup>22,37–39</sup> However, little is known about the pathogenic role of AOPPs. Our present study has illustrated the role of AOPPs in the pathogenesis of diabetes, which will help to understand the reason that oxidative stress persists in chronic diseases. It may provide new insight into the mechanism of oxidative stress-induced tissue injury and treatment of redox-associated diseases.

Increased levels of AOPPs in diabetic patients has been reported, although different studies presented different values.<sup>38,40–42</sup> Other than AOPPs, increased level of advanced glycation end products (AGEs), the products of nonenzymatic glycation/oxidation of proteins/lipids, was also reported and have deleterious effects on the function of pancreatic islets in type 2 diabetes mellitus.<sup>42–44</sup> AGEs formation is enhanced in diabetes by increased blood glucose, the production of small reactive carbonyl compounds such as glyoxal, and reactive aldehydes such as 4-hydroxynonenal.<sup>45</sup> AOPPs are structurally similar to AGEs and show biological activities as AGEs.<sup>44</sup> Notably, circulating AOPPs and AGEs levels in type 2 diabetes mellitus elderly subjects were related to low-density lipoprotein susceptibility to oxidation and nitric oxide metabolic pathway products. All these oxidative and glycoxidative stress markers were significantly higher in both prediabetic and diabetic subjects compared with healthy elderly individuals.<sup>40</sup> However, it remains to be seen whether AOPPs act in company with other oxidative and glycoxidative markers to destroy pancreatic  $\beta$ -cells in AOPPs-treated animals.

In conclusion, this is the first study to demonstrate that accumulation of AOPPs promotes  $\beta$ -cell destruction by the induction of  $\beta$ -cell apoptosis, which is mainly mediated by NADPH oxidase-dependent  $O_2^-$  generation. Given that AOPPs accumulation is prevalent in diverse pathophysiological conditions such as diabetes, metabolic syndrome, and chronic kidney disease, this finding might be highly significant because it will likely yield further insight into the pathogenic effects of AOPPs on islet, and may provide new targets for the prevention of  $\beta$ -cell destruction seen in these disorders and controlling the advance of diabetes.

Supplementary Information accompanies the paper on the Laboratory Investigation website (<http://www.laboratoryinvestigation.org>)

#### ACKNOWLEDGMENTS

This study was supported by the National Natural Science Foundation of China (Grant Nos. 81620108003 to FFH, 30971382 to ML, and 81270825 to AL).

#### DISCLOSURE/CONFLICT OF INTEREST

The authors declare no conflict of interest.

- Mazzone T. Hyperglycaemia and coronary heart disease: the meta picture. *Lancet* 2009;373:1737–1738.
- Yach D, Stuckler D, Brownell KD. Epidemiologic and economic consequences of the global epidemics of obesity and diabetes. *Nat Med* 2006;12:62–66.
- Luther JM, Brown NJ. The renin–angiotensin–aldosterone system and glucose homeostasis. *Trends Pharmacol Sci* 2011;32:734–739.
- Luo P, Wang MH. Eicosanoids,  $\beta$ -cell function, and diabetes. *Prostag Oth Lipid Mediat* 2011;95:1–10.
- Morgan D, Oliveira-Emolio HR, Keane D, *et al*. Glucose, palmitate and pro-inflammatory cytokines modulate production and activity of a phagocyte-like NADPH oxidase in rat pancreatic islets and a clonal  $\beta$ -cell line. *Diabetologia* 2007;50:359–369.
- Eldin WS, Ragheb A, Klassen J, *et al*. Evidence for increased risk of prediabetes in the uremic patient. *Nephron Clin Pract* 2008;108:c47–c55.
- Sui Y, Zhao HL, Ma RC, *et al*. Pancreatic islet  $\beta$ -cell deficit and glucose intolerance in rats with uninephrectomy. *Cell Mol Life Sci* 2007;64:3119–3128.
- Robertson RP. Chronic oxidative stress as a central mechanism for glucose toxicity in pancreatic islet Beta cells in diabetes. *J Biol Chem* 2004;279:42351–42354.
- Huang XJ, Wang X, Ihsan A, *et al*. Interactions of NADPH oxidase, renin–angiotensin–aldosterone system and reactive oxygen species in mequindox-mediated aldosterone secretion in Wistar rats. *Toxicol Lett* 2010;198:112–118.
- Jiao J, Dou L, Li M, *et al*. NADPH oxidase 2 plays a critical role in dysfunction and apoptosis of pancreatic  $\beta$ -cells induced by very low-density lipoprotein. *Mol Cell Biochem* 2012;370:103–113.
- Li M, Dou L, Jiao J, *et al*. NADPH oxidase 2-derived reactive oxygen species are involved in dysfunction and apoptosis of pancreatic  $\beta$ -cells induced by low density lipoprotein. *Cell Physiol Biochem* 2012;30:439–449.
- Newsholme P, Haber EP, Hirabara SM, *et al*. Diabetes associated cell stress and dysfunction: role of mitochondrial and non-mitochondrial ROS production and activity. *J Physiol* 2007;583:9–24.
- Zhang Z, Liew CW, Handy DE, *et al*. High glucose inhibits glucose-6-phosphate dehydrogenase, leading to increased oxidative stress and  $\beta$ -cell apoptosis. *FASEB J* 2010;24:1497–1505.
- Luciano Viviani G, Puddu A, Sacchi G, *et al*. Glycated fetal calf serum affects the viability of an insulin-secreting cell line *in vitro*. *Metabolism* 2008;57:163–169.
- Guo ZJ, Niu HX, Hou FF, *et al*. Advanced oxidation protein products activate vascular endothelial cells via a RAGE-mediated signaling pathway. *Antioxid Redox Signal* 2008;10:1699–1712.
- Atabek ME, Keskin M, Yazici C, *et al*. Protein oxidation in obesity and insulin resistance. *Eur J Pediatr* 2006;165:753–756.
- Korkmaz GG, Altinoglu E, Civelek S, *et al*. The association of oxidative stress markers with conventional risk factors in the metabolic syndrome. *Metabolism* 2013;62:828–835.
- Martin-Gallan P, Carrascosa A, Gussinye M, *et al*. Biomarkers of diabetes-associated oxidative stress and antioxidant status in young diabetic patients with or without subclinical complications. *Free Radical Bio Med* 2003;34:1563–1574.
- Oberg BP, McMenamin E, Lucas FL, *et al*. Increased prevalence of oxidant stress and inflammation in patients with moderate to severe chronic kidney disease. *Kidney Int* 2004;65:1009–1016.
- Witko-Sarsat V, Friedlander M, Nguyen Khoa T, *et al*. Advanced oxidation protein products as novel mediators of inflammation and monocyte activation in chronic renal failure. *J Immunol* 1998;161:2524–2532.
- Li HY, Hou FF, Zhang X, *et al*. Advanced oxidation protein products accelerate renal fibrosis in a remnant kidney model. *J Am Soc Nephrol* 2007;18:528–538.

22. Shi XY, Hou FF, Niu HX, *et al*. Advanced oxidation protein products promote inflammation in diabetic kidney through activation of renal nicotinamide adenine dinucleotide phosphate oxidase. *Endocrinology* 2008;149:1829–1839.
23. Cao W, Xu J, Zhou ZM, *et al*. Advanced oxidation protein products activate intrarenal renin-angiotensin system via a CD36-mediated, redox-dependent pathway. *Antioxid Redox Signal* 2013;18:19–35.
24. Liu B, Hou X, Zhou Q, *et al*. Detection of advanced oxidation protein products in patients with chronic kidney disease by a novel monoclonal antibody. *Free Radical Res* 2011;45:662–671.
25. Roma LP, Pascal SM, Duprez J, *et al*. Pancreatic islet cell apoptosis and insulin secretory defects after prolonged culture in a low non-stimulating glucose concentration. *Diabetologia* 2012;55:2226–2237.
26. Su ZX, Zhu HG, Zhang MH, *et al*. Salt-induced changes in cardiac phosphoproteome in a rat model of chronic renal failure. *PLoS ONE* 2014;9:e100331.
27. Bindom SM, Hans CP, Xia H, *et al*. Angiotensin I-converting enzyme type 2 (ACE2) gene therapy improves glycemic control in diabetic mice. *Diabetes* 2010;59:2540–2548.
28. Piro S, Anello M, Di Pietro C, *et al*. Chronic exposure to free fatty acids or high glucose induces apoptosis in rat pancreatic islets: possible role of oxidative stress. *Metabolism* 2002;51:1340–1347.
29. Iwao Y, Nakajou K, Nagai R, *et al*. CD36 is one of important receptors promoting renal tubular injury by advanced oxidation protein products. *Am J Physiol Renal Physiol* 2008;295:F1871–F1880.
30. Wei XF, Zhou QG, Hou FF, *et al*. Advanced oxidation protein products induce mesangial cell perturbation through PKC-dependent activation of NADPH oxidase. *Am J Physiol Renal Physiol* 2009;296:F427–F437.
31. Ping M, Xiao W, Mo L, *et al*. Paeonol attenuates advanced oxidation protein product-induced oxidative stress injury in THP-1 macrophages. *Pharmacology* 2014;93:286–295.
32. Oliveira HR, Verlengia R, Carvalho CR, *et al*. Pancreatic  $\beta$ -cells express phagocyte-like NAD(P)H oxidase. *Diabetes* 2003;52:1457–1463.
33. Guichard C, Moreau R, Pessayre D, *et al*. NOX family NADPH oxidases in liver and in pancreatic islets: a role in the metabolic syndrome and diabetes? *Biochem Soc Trans* 2008;36:920–929.
34. Hirata AE, Morgan D, Oliveira-Emilio HR, *et al*. Angiotensin II induces superoxide generation via NAD(P)H oxidase activation in isolated rat pancreatic islets. *Regul Peptides* 2009;153:1–6.
35. Morgan D, Rebelato E, Abdulkader F, *et al*. Association of NAD(P)H oxidase with glucose-induced insulin secretion by pancreatic  $\beta$ -cells. *Endocrinology* 2009;150:2197–2201.
36. Román CL, Flores LE, Maiztegui B, *et al*. Islet NADPH oxidase activity modulates  $\beta$ -cell mass and endocrine function in rats with fructose-induced oxidative stress. *Biochim Biophys Acta* 2014;1840:3475–3482.
37. Zhou LL, Hou FF, Wang GB, *et al*. Accumulation of advanced oxidation protein products induces podocyte apoptosis and deletion through NADPH dependent mechanisms. *Kidney Int* 2009;76:1148–1160.
38. Piwowar A, Knapik-Kordecka M, Szczecińska J, *et al*. Plasma glycooxidation protein products in type 2 diabetic patients with nephropathy. *Diabetes Metab Res Rev* 2008;24:549–553.
39. Liu SX, Hou FF, Guo ZJ, *et al*. Advanced oxidation protein products accelerate atherosclerosis through promoting oxidative stress and inflammation. *Arterioscler Thromb Vasc Biol* 2006;26:1156–1162.
40. Gradinarua D, Borsa C, Ionescu C, *et al*. Advanced oxidative and glycooxidative protein damage markers in the elderly with type 2 diabetes. *J Proteomics* 2013;92:313–322.
41. Esteghamati A, Eskandari D, Mirmiranpour H, *et al*. Effects of metformin on markers of oxidative stress and antioxidant reserve in patients with newly diagnosed type 2 diabetes: a randomized clinical trial. *Clin Nutr* 2013;32:179–185.
42. Kalousova M, Skrha J, Zima T. Advanced glycation end-products and advanced oxidation protein products in patients with diabetes mellitus. *Physiol Res* 2002;51:597–604.
43. Robertson RP, Harmon J, Tran POT, *et al*.  $\beta$ -Cell glucose toxicity, lipotoxicity, and chronic oxidative stress in type 2 diabetes. *Diabetes* 2004;53:S119–S124.
44. Tsukahara H, Sekine K, Uchiyama M, *et al*. Formation of advanced glycosylation end products and oxidative stress in young patients with type 1 diabetes. *Pediatr Res* 2003;54:419–424.
45. Turk Z. Glycotoxines, carbonyl stress and relevance to diabetes and its complications. *Physiol Res* 2010;59:147–156.